Room-Temperature Ferromagnetism in Transparent Transition Metal–Doped Titanium Dioxide

**Yuji Matsumoto,[1] Makoto Murakami,[1] Tomoji Shono,[1]
Tetsuya Hasegawa,[1] Tomoteru Fukumura,[2] Masashi Kawasaki,[2]
Parhat Ahmet,[3] Toyohiro Chikyow,[3,4] Shin-ya Koshihara,[5]
Hideomi Koinuma[1,3,6,7]***

Dilute magnetic semiconductors and wide gap oxide semiconductors are appealing materials for magnetooptical devices. From a combinatorial screening approach looking at the solid solubility of transition metals in titanium dioxides and of their magnetic properties, we report on the observation of transparent ferromagnetism in cobalt-doped anatase thin films with the concentration of cobalt between 0 and 8%. Magnetic microscopy images reveal a magnetic domain structure in the films, indicating the existence of ferromagnetic long-range ordering. The materials remain ferromagnetic above room temperature with a magnetic moment of 0.32 Bohr magnetons per cobalt atom. The film is conductive and exhibits a positive magnetoresistance of 60% at 2 kelvin.

Ferromagnetic semiconductors (FS) obtained by doping magnetic impurities into host semiconductors, mostly III-V (*1*) and II-VI (*2*) compounds, are key materials for spin electronics in which the correlation between charge and spin of electrons is used to bring about spin-dependent electronic functionality such as giant magnetoresistance and spin field effect transistor. Among the materials so far reported, Mn-doped GaAs has the highest Curie temperature, T_C, ~100 K, and is presumed to be a promising candidate for practical applications. Following the theoretical prediction that ZnO would become ferromagnetic by doping with 3d transition elements (*3*), intensive experimental work has begun on dilute magnetic oxides (DMO). Although magnetoresistance was observed in some 3d-doped ZnO films (*4*, *5*), no sign of ferromagnetism has yet been observed.

Titanium dioxide, TiO_2, has been extensively studied for its unique physical and chemical properties, such as high refractive index, excellent optical transmittance in the visible and near-infrared region, high dielectric constant (*6*), and photocatalysis for water cleavage (*7*), but there has been no report of its use as a DMO. TiO_2 has three kinds of crystal structure, rutile, anatase, and brookite, composed of Ti ions having octahedral coordination. They are wide gap oxide semiconductors and used as an electrode in electrochemistry. In addition, anatase has high mobility of n-type charge carrier and large thermopower of –200 μV/K at 300 K (*8*). However, because anatase is not as thermodynamically stable as rutile, the pure anatase phase with high crystallinity is difficult to obtain in a bulk process. For thin films, on the other hand, appropriate choice of substrate material has enabled us to grow anatase films with high crystallinity (*9*). We report on the discovery of ferromagnetism in the Co-doped anatase $Ti_{1-x}Co_xO_2$ that was found in a combinatorial thin film library of anatase TiO_2 doped with various 3d transition metals.

$LaAlO_3$(001) and $SrTiO_3$(001) single crystals were used as substrates (*10*). To observe systematic changes of film properties as a function of doping level, we fabricated a combinatorial library integrating nine $Ti_{1-x}Co_xO_2$ films with different x values on a single substrate by the combinatorial laser molecular beam epitaxy technique (*11*) in 1×10^{-5} to 1×10^{-6} torr of oxygen at 950 to 1000 K. TiO_2 and Co-doped $Ti_{0.5}Co_{0.5}O_2$ ceramic targets were ablated with KrF excimer laser pulses (248 nm) that were synchronized with the rotational motion of combinatorial masks. The details of the combinatorial procedure have been described elsewhere (*11*). The Co contents in a series of $Co_x Ti_{1-x}O_2$ films were determined by electron probe microanalysis.

In the x-ray diffraction (XRD) pattern of a Co-doped TiO_2 film with $x = 0.08$ (Fig. 1A), only the (004) and (008) peaks of the anatase phase were observed, and the change of the lattice constant followed Vegard's law, as shown in the inset. Moreover, transmission electron microscope (TEM) observations (Fig. 1B) indicate no sign of segregation of impurity phases in the Co/Ti compositional range of $x < 0.08$; the lattice image and diffraction pattern of Co-doped anatase are identical to those of pure ($x = 0$) anatase. From these XRD and TEM results, it is concluded that a sizable amount of Co, at least up to $x = 0.08$, is soluble, i.e., homogeneously distributed in anatase. Probably because of the quasi-equilibrium nature of laser molecular beam epitaxy, the formation of $CoTiO_3$ and $CoTi_2O_5$, which are known to exist in the bulk Co-Ti-O phase diagram, was not observed.

A series of magnetic images were taken by a scanning superconducting quantum interference device (SQUID) microscope at 3 K for anatase films with different Co contents ($x = 0$ to 0.06) on a combinatorial chip (Fig. 2). In all of the Co-doped films, magnetic domain structures of around 20 μm in size can be seen. The pure TiO_2 ($x = 0$) film and the $LaAlO_3$ substrate do not show any magnetic structure within an experimental error of ~0.5 μT, consistent with the report by Chauvet *et al.* (*12*). With increasing Co content in the film, the magnitude of the magnetic field is systematically enhanced as a result of the increased spontaneous magnetization. These observations show that ferromagnetic long-range order emerges in the Co-doped TiO_2 anatase phase. We observed no sign of such ferromagnetic behavior in any other combinatorial TiO_2 film chips, either in the anatase or rutile phase, in which transition metals were solid soluted.

The magnetic response was measured as a function of magnetic field strength (H) (Fig. 3) for the $x = 0.07$ film on $SrTiO_3$(001) at room temperature, where the magnetic field was applied parallel to the film surface. Hysteresis is observed (Fig. 3A), indicating that the Co-doped anatase film is ferromagnetic even at room temperature. Spontaneous magnetic moment per Co atom was deduced from the saturated magnetization (M) value to be 0.32 μ_B. From the M-temperature (T) curve in a field of 20 mT applied parallel to the surface (Fig. 3B), T_C is estimated to be higher than 400 K, substantially higher than the values (<100 K) reported so far for other 3d-doped FS (*1*).

The optical properties of $Ti_{1-x}Co_xO_2$ anatase film are good, with the film remaining

---

[1] Ceramics Materials and Structures Laboratory, Tokyo Institute of Technology, Yokohama 226-8503, Japan. [2] Department of Innovative and Engineered Materials, Tokyo Institute of Technology, Yokohama 226-8502, Japan. [3] National Institute for Research in Inorganic Materials, 1-1 Namiki, Tsukuba, Ibaraki 305-0044, Japan. [4] National Research Institute for Metals, 1-2-1 Sengen, Tsukuba, Ibaraki, 305-0047, Japan. [5] Department of Materials Science, Tokyo Institute of Technology, 2-12-1 Okayama, Meguro-ku, Tokyo, Japan, and Kanagawa Academy of Science and Technology, KSP East Building 301, 3-2-1 Sakado, Takatsu-ku, Kawasaki-shi, Kanagawa, 213-0012, Japan. [6] Frontier Collaborative Research Center, Tokyo Institute of Technology, Yokohama 226-8503, Japan. [7] CREST-Japan Science and Technology, Waseda University, 55th Building, 3-4-1 Ohkubo, Shinjyuku-ku 169-8555, Japan.

*To whom correspondence should be addressed. E-mail: koinuma@oxide.rlem.titech.ac.jp

Fig. 1. (**A**) An XRD pattern of a Co-doped TiO_2 film (x = 0.08) showing (004) and (008) peaks of anatase without any impurity peaks. The c-axis length increased monotonously with increasing Co content following Vegard's low (inset). (**B**) Atomic resolution TEM image of a Co-doped TiO_2 film. No segregation of impurity phases was observed in the film.

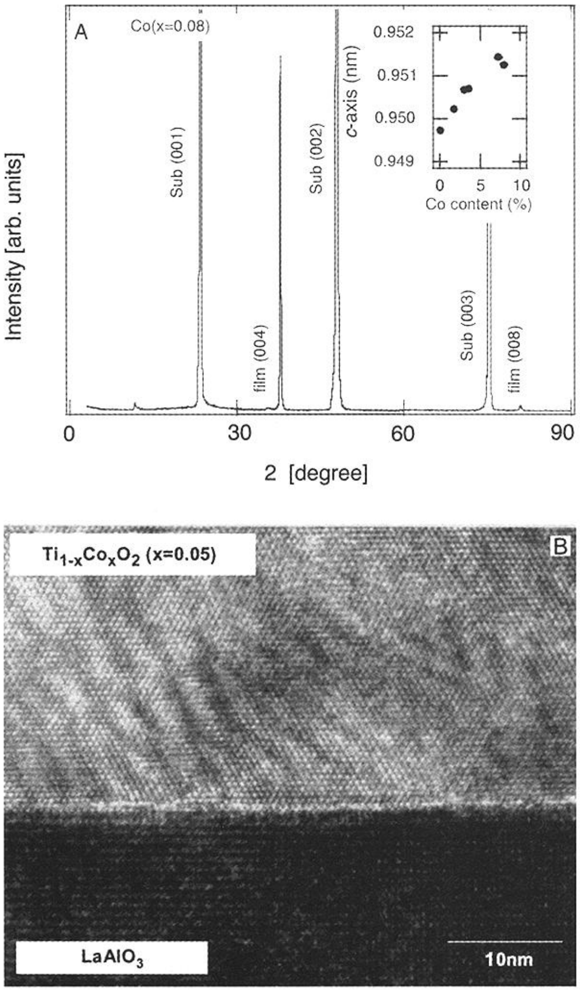

Fig. 2. A series of scanning SQUID microscope images (200 μm by 200 μm) taken at 3 K for anatase thin films with different Co contents on a combinatorial chip. (**A**) $x = 0$, (**B**) $x = 0.02$, (**C**) $x = 0.03$, and (**D**) $x = 0.06$. Magnetic domain structures were observed in all doped films, suggesting the presence of long-range ordering of magnetic moments induced by Co doping in the anatase thin film.

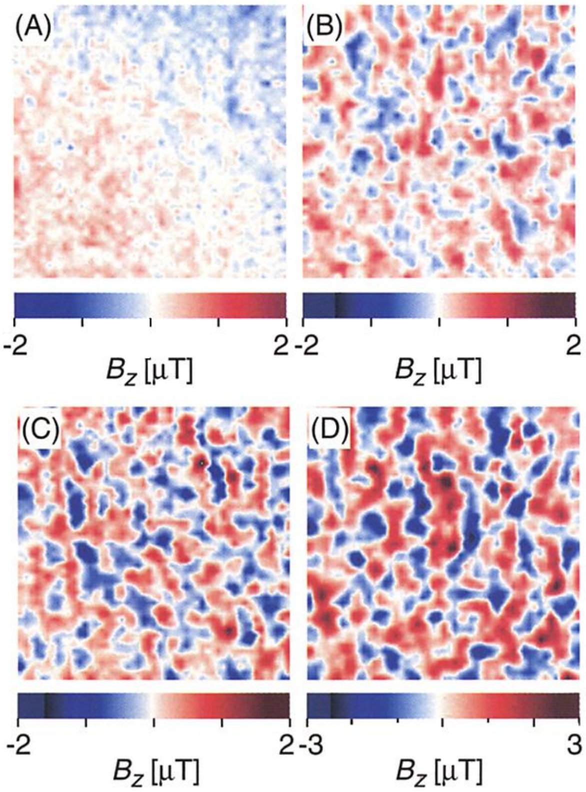

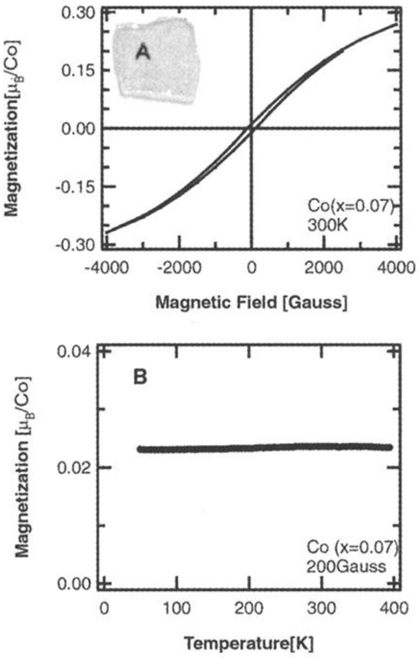

Fig. 3. (**A**) An M-H curve of an x = 0.07 film on $SrTiO_3$ taken at room temperature. Magnetic field was applied parallel to the film surface. Hysteresis is observed, indicating that the Co-doped anatase film is ferromagnetic even at room temperature. The film is transparent enough in the visible and near-infrared region to make the background letter (A) visible (inset). (**B**) An M-T curve in a field of 20 mT parallel to the surface. T_C is estimated to be higher than 400 K.

transparent in the visible and near-infrared regions and exhibiting a band gap at 400 nm (3.1 eV). The transparency is demonstrated by the clear image of letter A, which is placed beneath a $Ti_{1-x}Co_xO_2$ (x = 0.06) film on $LaAlO_3$ substrate (inset of Fig. 3A). Different from two ferromagnetic materials, $FeBO_3$ and FeF_3, that were reported to be transparent but green in color (*13*), the Co-doped anatase is colorless and has appreciable conductivity. The resistivity and carrier concentration of the $Co_xTi_{1-x}O_2$ film are about 0.1 to 1 ohm·cm and $10^{18}/cm^3$, respectively, at room temperature, being scarcely dependent on the Co doping level. The ferromagnetic $Co_xTi_{1-x}O_2$ film (x = 0.07) on $LaAlO_3$ exhibits a positive magnetoresistance (MR) of as much as 60% at 2 K in a field of 8 T applied normal to the surface (Fig. 4) and represents an observation of MR in anatase films.

The mixing of granular precipitates of magnetic materials, Co clusters for instance, can be a reason for the observed spontaneous magnetism (*14*, *15*). Although the possibility cannot be completely ruled out at present, the XRD and TEM measurements show no sign of such metal granules as mentioned before. If the clustering of cobalt occurred, we should have observed such granules in TEM image as were reported by Mitani *et al.* (*15*).

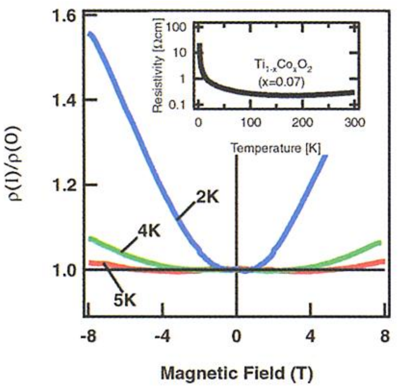

Fig. 4. The MR measurements of the $x = 0.07$ specimen in the temperature range of 2 to 5 K. A positive MR = 60% is observed at 2 K in a field of 8 T applied normal to the surface. The temperature dependence of the resistivity is also shown (inset).

Assuming that thermal equilibrium is reached in our growth conditions, the valence state of Co ions should be either Co^{2+} or Co^{3+}, in view of the facts that the films were deposited at 950 to 1000 K and cooled down to 500 K in 1×10^{-6} to 1×10^{-5} torr of oxygen (*16*). If Co ions are in high spin state, we expect S to vary from 3/2 to 4/2, depending on the mixing ratio of Co^{2+} and Co^{3+} in the film, giving a spontaneous magnetic moment m_{sp} between 3 and 4 μ_B/Co. Meanwhile, the low spin states of Co^{2+} and Co^{3+} yield at most $S = 1/2$ ($m_{sp} = 1$ μ_B/Co). The low spin configuration of Co ions is thus consistent with the observed magnetic moment in the M-H curve in Fig. 3A. In other words, the ferromagnetism of Co-TiO_2 is attributable to the local spins of Co ions.

X.-D. Xiang and co-workers reported magnetoresistance but not ferromagnetism in a class of $LnMCoO_3$ (Ln = Y or La; M = Sr, Ca, or Ba) (*17*). The anatase structure can be viewed as a stacking of TiO_2 B-site layers along the c axis in perovskite. From the viewpoint of this structural similarity between $LnMCoO_3$ and Co-doped TiO_2, the origins of these two magnetic effects may be related. The results reported here are rather serendipitous, and the underlying microscopic mechanism of long-range order is still an open question at present.

References and Notes

1. H. Ohno, *Science* **281**, 951 (1998).
2. J. K. Furdyna, *J. Appl. Phys.* **64**, R29 (1998).
3. T. Fukumura, Z. W. Jin, A. Ohtomo, H. Koinuma, M. Kawasaki, *Appl. Phys. Lett.* **75**, 3366 (2000).
4. K. Sato, H. K. Yoshida, *Jpn. J. Appl. Phys.* **39**, L555 (2000).
5. Z. W. Jin *et al.*, in preparation.
6. H. Kim *et al.*, *Appl. Phys. Lett.* **69**, 25 (1996).
7. A. Fujishima, K. Honda, *Nature* **238**, 37 (1972).
8. L. Forro *et al.*, *J. Appl. Phys.* **75**, 633 (1994).
9. Y. Matsumoto *et al.*, *SPIE Proc.* **3941**, 19 (2000).
10. M. Murakami *et al.*, in preparation.
11. Y. Matsumoto *et al.*, *Jpn. J. Appl. Phys.* **38**, L603 (1999).
12. O. Chauvet, L. Forro, I. Kos, M. Miljak, *Solid State Commun.* **93**, 667 (1995).
13. R. Wolfe, A. J. Kurtzig, R. C. LeCraw, *J. Appl. Phys.* **41** (no. 3), 1218 (1970).
14. J. Q. Xiao, J. S. Jiang, C. L. Chien, *Phys. Rev. Lett.* **68**, 3749 (1992).
15. S. Mitani, H. Fujimori, S. Ohnuma, *J. Magn. Magn. Mater.* **165**, 141 (1997).
16. M. W. Chase Jr. *et al.*, *J. Phys. Chem. Ref. Data* **14**, suppl. no. 1 (1985).
17. G. Briceño *et al.*, *Science* **270**, 273 (1995).
18. The authors express their thanks for financial support from the Comet project of Science and Technology Agency in Japan as well as from the Japan Society for the Promotion of Science.

28 September 2000; accepted 18 December 2000
Published online 11 January 2001; 10.1126/science.1056186
Include this information when citing this paper.

First Solvation Shell of the Cu(II) Aqua Ion: Evidence for Fivefold Coordination

Alfredo Pasquarello,[1,2]* Ingrid Petri,[3] Philip S. Salmon,[3] Olivier Parisel,[1,2] Roberto Car,[1,4] Éva Tóth,[5] D. Hugh Powell,[6] Henry E. Fischer,[7] Lothar Helm,[5] André E. Merbach[5]

We determined the structure of the hydrated Cu(II) complex by both neutron diffraction and first-principles molecular dynamics. In contrast with the generally accepted picture, which assumes an octahedrally solvated Cu(II) ion, our experimental and theoretical results favor fivefold coordination. The simulation reveals that the solvated complex undergoes frequent transformations between square pyramidal and trigonal bipyramidal configurations. We argue that this picture is also consistent with experimental data obtained previously by visible near-infrared absorption, x-ray absorption near-edge structure, and nuclear magnetic resonance methods. The preference of the Cu(II) ion for fivefold instead of sixfold coordination, which occurs for other cations of comparable charge and size, results from a Jahn-Teller destabilization of the octahedral complex.

Copper is one of the most abundant transition elements in biological systems, with an occurence of 80 to 120 mg in a normal human body (*1*), but the behavior of its simplest aqueous form, the Cu(II) ion, remains poorly understood. Because of its electronic d^9 configuration, a Jahn-Teller distortion is generally assumed to axially elongate two bonds of the octahedral $[Cu(H_2O)_6]^{2+}$ complex (*2*–*15*), yielding an unusually fast water exchange rate (*13*, *15*). In addition, an even shorter time scale has been observed and has been attributed to rapid transformations between configurations differing by the orientation of the elongation (*14*, *15*). However, validation of this model suffers from the experimental difficulties associated with measuring the axial Cu-O bond lengths (*2*–*12*)

The nearest-neighbor Cu-O bond lengths in aqueous solution are well characterized by a variety of experimental techniques such as x-ray diffraction (*2*–*4*), extended x-ray absorption fine structure (EXAFS) (*5*–*9*), x-ray absorption near-edge structure (XANES) (*7*, *8*), and isotopic substitution in neutron diffraction (*10*–*12*), all of which provide consistent values in the 1.94 to 2.00 Å range. By contrast, the more distant axial bond lengths have so far eluded accurate determination, as manifested by the large interval over which the measured values are spread (2.12 to 2.60 Å) (*12*). These problems stem at least partly from the fact that x-ray diffraction, EXAFS, and XANES measurements all require fitting procedures that incorporate a priori assumptions about the structure (*2*–*9*) and that first-difference pair distribution functions obtained by neutron diffraction cannot discern axial Cu-O from overlapping Cu-H correlations (*10*–*12*).

We have undertaken a combined experimental and theoretical investigation to unveil the detailed structure and dynamics of the hydrated Cu(II) complex in aqueous solution. We applied the second-difference isotopic substitution method in neutron diffraction

---

[1]Institut Romand de Recherche Numérique en Physique des Matériaux (IRRMA), PPH-Ecublens, CH-1015 Lausanne, Switzerland. [2]Ecole Polytechnique Fédérale de Lausanne (EPFL), PPH-Ecublens, CH-1015 Lausanne, Switzerland. [3]Department of Physics, University of Bath, Bath BA2 7AY, UK. [4]Department of Chemistry and Princeton Materials Institute, Frick Chemical Laboratory, Washington Road, Princeton University, Princeton, NJ 08544, USA. [5]Institut de Chimie Minérale et Analytique, Université de Lausanne, Bâtiment de chimie, CH-1015 Lausanne-Dorigny, Switzerland. [6]Department of Chemistry, Durham University, Durham DH1 3LE, UK. [7]Laboratoire pour l'Utilisation du Rayonnement Electromagnétique (LURE), Bâtiment 209d, Centre Universitaire Paris-Sud, Boîte Postale 34, F-91898 Orsay Cédex, France.

*To whom correspondence should be addressed. E-mail: Alfredo.Pasquarello@epfl.ch